Lipid degradation contributes to flavor formation during air-dried camel jerky processing

Shenyi Cao, Yinghua Fu[*]

Xinjiang Key Laboratory of Biological Resources and Genetic Engineering, College of Life Science and Technology, Xinjiang University, Urumqi, Xinjiang 830017, China

ARTICLE INFO

ABSTRACT

Lipids play an important role in flavor formation in meat products. To determine the contribution of lipids to flavor formation during air-dried camel jerky processing, lipid changes were analyzed by UHPLC-Q-Exactive Orbitrap MS/MS in this study, and volatile compounds were identified by HS-SPME-GC-ToF-MS. Results showed that 606 lipid molecules belonging to 30 subclasses were identified and 206 differential lipid molecules were screened out (VIP > 1, $P < 0.05$); Cer/NS (d18:1/20:0), LPE (18:1), FA (18:0), GlcADG (12:0/24:1), and PE (18:2e/22:5) were identified as potential lipid biomarkers. A total of 96 volatile compounds were also identified, and 16 of these were identified as key aroma compounds in air-dried camel jerky. Meanwhile, 11 differential lipids significantly, negatively correlated with 7 key aroma compounds ($P < 0.05$) during processing, indicating that the precursors produced by the degradation of lipid molecules were important sources of volatile flavor substances in air-dried camel jerky.

1. Introduction

Camel meat serves as the main red meat for consumption in semi-arid and arid areas (Baba et al., 2021). The Bactrian camel is an indispensable livestock resource in China, which number in Xinjiang accounts for 48.92% of the total in China. Camel meat has a high nutritional value as it has a higher water, mineral, vitamin and amino acid contents than mutton, beef, and chicken (Hamed Hammad Mohammed et al., 2020). Nowadays, camel meat is appreciated by consumers as healthy food, because of its lower total fat and cholesterol contents, higher poly-unsaturated fatty acid (PUFA) content, and higher oleic acid (Abdelhadi et al., 2017). For instance, the proportions of PUFA contents and of linoleic acid and linolenic acid combined in the *biceps femoris* of camel muscle were 12.82% and about 14.70% respectively (Kadim et al., 2013).

Dry-curing and air-drying were widely used globally in meat products processing, and contributed unique jerky flavor. In recent years, there have been numerous studies on the effect of substance changes on product quality during the processing of air-dried meat products. García-García et al. (2018) reported that compositional changes related to ripening of dry-fermented sausage were monitored through the NMR spectra. Protein changes have impact on the flavor development and texture of drying meat. Poljanec et al. (2021) monitored that proteolysis

and protein oxidation during the smoked dry-cured ham processing, and the results showed a strong relationship between protein oxidation and proteolysis. Lipid degradation, transformation and oxidation during drying underlie changes in lipid content and metabolites. For example, lipidomics was applied to determine lipid changes during shrimp drying, which results showed that PEs and PCs containing unsaturated fatty acids decreased after drying, while those containing SFAs and MUFAs increased (Zhao et al., 2022). Also, the production of volatile flavor compounds is influenced by lipid type and content. The generation of alcohols and esters was identified to be related to changes in tri-glycerides and phosphatidylcholine containing PUFA (Zhang et al., 2023). Likewise, the generation of heptanal, octanal, nonanal, 2,3-glutaraldehyde and 3-hydroxy-2-butanone were reported to have correlated with oleic acid, linoleic acid and stearic acid, and their amounts increased with the degree of oxidation (Huang et al., 2022).

Lipidomics is a promising tool for identifying lipids and screening potential markers during meat processing. Shotgun lipidomics was applied to measure the composition and changes in phospholipids during the processing of ducks and further, to screen molecular markers which could be used to distinguish different operating units in water-boiled salted duck (Li et al., 2020). Also, lipidomics based on UPLC-ESI-MS/MS was used to screen key lipids for binding and generating aroma compounds, which served as potential markers for the

---

discrimination of roasted mutton (Liu et al., 2022). Also, the lipid composition and lipid-related metabolic pathways during golden pomfret fermentation were identified by employing UHPLC-MS/MS based untargeted lipidomic analysis. In addition, volatile compounds in meat and meat products were identified by gas chromatography (Wang, Wu, et al., 2022). Correlation analysis between differential lipids and odors from sturgeon surimi, showed that glycerol phospholipid oxidation contributed to flavor formation (Xu et al., 2023).

In Xinjiang, air-dried camel jerky is a traditional cured meat product that is popular throughout the region due to its unique taste. However, there is lack of standardization during industrial production of air-dried camel jerky. Flavor is one of the most important quality characteristics of meat products, and lipids are important precursors for the flavor formation in meat products. Therefore, in the study, UHPLC-Q-Exactive Orbitrap MS/MS was used to analyze lipid changes and identify key differential lipids, HS-SPME-GC-ToF-MS was used to identify the key aroma compounds during air-dried camel jerky processing. Meanwhile, correlations between volatile flavor compounds and lipid metabolites were analyzed to reveal the mechanism of flavor formation in air-dried camel jerky. The results of the study could provide a scientific basis for the control of flavor quality, standardization and industrial production of air-dried camel jerky.

2. Materials and methods

2.1. Preparation of air-dried camel jerky

In previous study, the process of air-dried camel jerky was optimized by single factors such as the air-drying time, salt addition and curing time, and response surface methodology. According to the results, the optimal condition of air-dried camel jerky process was air-drying time of 8 d, salt addition of 2.6%, and curing time of 3 d.

In the study, three Xinjiang Bactrian camels (2-year-old, male) were acquired from Miquan in Xinjiang, China. Meat samples from the hind shank were obtained and transported to the laboratory under 4 °C within 2 h. Following pre-cooling for 24 h at 4 °C, the skin, fascia and fat of the meat were removed and the meat then cut into strips (10–15 cm × 5 cm × 3 cm). The meat strips were manually rubbed with salt (2.5% of the weight of the meat) until the salt dissolved and stored for 3 days at 0–4 °C and 85–95% RH. After salting, they were air-dried at 4–8 °C and 45–55% RH for 8 days (in a constant temperature and humidity room). Six camel jerky samples were selected during each processing stage, resulting in a total of 36 camel jerky for experimental analysis. The six groups included raw camel meat (S1), cured for 3 d (S2), air-dried for 2 d (S3), 4 d (S4), 6 d (S5), and 8 d (S6).

2.2. Chemicals

Methanol (CAS: 67–56-1, purity: LC-MS grade), acetonitrile (CAS: 75–05-8, purity: LC-MS grade), MTBE (CAS: 1634-04-4, purity: LC-MS grade), ammonium formate (CAS: 540–69-2, purity: LC-MS grade), dichloromethane (CAS: 75–09-2, purity: LC-MS grade) were purchased from CNW Technologies. Isopropanol (CAS: 67–63-0, purity: LC-MS grade) was purchased from Fisher Chemical. 2-Octanol (CAS: 6169-06-8, purity≥99.5%) was purchased from TCL.

2.3. UHPLC-Q-extractive Orbitrap MS/MS analysis

Frozen camel jerky samples were ground to powder. Proportions of each sample was weighed (25 mg) into Eppendorf tubes, and 200 μL of water, 480 μL of extraction solution (MTBE:MeOH = 5:1) was added sequentially. The samples were vortexed for 30 s, then were homogenized at 35 Hz for 4 min and sonicated in an ice-water bath for 5 min, which were repeated three times. Then the samples were incubated at −40 °C for 1 h and centrifuged at 3000 rpm for 15 min at 4 °C. Volumes of supernatants (300 μL) were transferred to fresh tubes and dried in a

vacuum concentrator at 37 °C. After, the dried samples were reconstituted in 100 μL of solution (DCM:MeOH = 1:1) by sonication for 10 min in an ice-water bath. The constitution was then centrifuged at 13000 rpm for 15 min at 4 °C, and 75 μL of supernatant was transferred to a fresh glass vial for LC-MS/MS analysis. The quality control sample was prepared by mixing an equal aliquot of the supernatants (20 μL) from all the samples.

LC-MS/MS analyses were performed using an UHPLC system (1290, Agilent Technologies, Santa Clara, CA, USA), equipped with a Kinetex C18 column (2.1 × 100 mm, 1.7 μm, Phenomen, Torrance, CA, USA). The mobile phase A consisted of 40% water, 60% acetonitrile, and 10 mmol/L ammonium formate. The mobile phase B consisted of 10% acetonitrile and 90% isopropanol, to which 50 mL of 10 mmol/L ammonium formate was added for every 1000 mL mixed solvent. The elution gradient was 40% B from 0 to 1.0 min, 40%–100% B from 1.0 to 12.0 min, 100% B from 12.0 to 13.5 min, 100%–40% B from 13.5 to 13.7 min, 40% B from 13.7 to 18.0 min. The flow rate was set at 0.3 mL/min, and the column temperature was 55 °C. The auto-sampler temperature was 4 °C, and the injection volume was 2 μL (positive) or 2 μL (negative), respectively. The QE mass spectrometer was used for its ability to acquire MS/MS spectra on data-dependent acquisition (DDA) mode in the control of the acquisition software (Xcalibur 4.0.27, Thermo, Waltham, MA, USA). The ESI source conditions were: sheath gas flow rate as 30 Arb, Aux gas flow rate as 10 Arb, capillary temperature 320 °C (positive),300 °C (negative), full MS resolution as 70,000, MS/MS resolution as 17,500, collision energy as 15/30/45 in NCE mode, and spray voltage as 5 kV (positive) or − 4.5 kV (negative).

2.4. GC-ToF-MS analysis

A proportion of the meat sample (5.0 g) was placed into a 20 mL headspace bottle, to which 10 μL of 2-octanol (10 mg/L stock in dH₂O) was added as internal standard. After pre-heating at 60 °C for 15 min, the sample was incubated at 60 °C for 30 min by SPME fiber (50130um DVB/CAR/PDMS, Stableflex (2 cm) 23Ga, Autosampler, 3pk (Gray-Notched)), and then desorbed at 250 °C for 4 min. GC-ToF-MS analysis was performed using the 7890 gas chromatograph system (Agilent Technologies, Santa Clara, CA, USA) equipped with DB-Wax column (30 m × 250 μm × 0.25 μm, Agilent Technologies, Santa Clara, CA, USA) and 5977B mass spectrometer (Agilent Technologies, Santa Clara, CA, USA). The system injected in splitless mode. Helium was used as the carrier gas. The front inlet purge flow was 3 mL/min, and the gas flow rate through the column was 1 mL/min. The initial temperature was maintained at 40 °C for 4 min, raised to 245 °C at a rate of 5 °C/min, and kept for 5 min. The injection, transfer line, ion source and quad temperatures were 250, 250, 230 and 150 °C, respectively. The energy was −70 eV in electron impact mode. The mass spectrometry data were acquired in scan mode with the m/z range of 20–400, and solvent delay of 0 min.

2.5. Relative odor activity value

The relative odor activity value (ROAV) was used to evaluate the contribution of individual compounds to the overall aroma. Following Fang et al. (2022), the ROAV of the volatile flavor compound with the greatest flavor contribution was set as $ROAV_{stan} = 100$, and that for other volatile compounds was calculated as follows:

$$ROAV_n \approx 100 \times \frac{C_{n\%}}{Cs_{tan\%}} \times \frac{C_{stan}}{T_n}$$

$C_{stan\%}$ and T_{stan} were the relative percentage content of compounds that contribute the most and the corresponding sensory threshold, respectively. $C_{n\%}$ and T_n were the relative percentage content of each volatile compound and the corresponding sensory threshold, respectively.

2.6. Data preprocessing and annotation

The raw data files obtained were converted to the mzXML format using the 'msconvert' program from ProteoWizard (Palo Alto, CA, USA). The CentWave algorithm in XCMS was used for peak detection, extraction, alignment, and integration; the minfrac for annotation was set at 0.5 and the cut-off for annotation was set at 0.3. Lipids were identified through spectral matches using the LipidBlast library, which was developed using R and based on XCMS.

The chroma TOF 4.3× software (LECO Corporation, St. Joseph, MI, USA) and NIST.14 database (Gaithersburg, MD, USA) were used for raw peaks exacting, the data baselines filtering and calibration of the baseline, peak alignment, deconvolution analysis, peak identification, integration and spectrum match of the peak area. Compounds with a similarity index higher than 80 were selected as the compounds present in the sample.

2.7. Statistical analysis

Statistical analyses were performed using SPSS 25.0 (SPSS, Inc., Chicago, IL, USA). Student *t*-test was used in the statistical evaluation of the results. Principal component analysis (PCA) and orthogonal projections to latent structures discriminant analysis (OPLS-DA) were conducted using self-written R software package (Biotree, Shanghai, China), based on SIMCA (Sartorius Stedim Data Analytics AB, Umea, Sweden). Origin 2021 (OriginLab Corporation, Northampton, MA, USA) was used to generate the graphs. Data were expressed as mean ± standard error.

3. Results

3.1. Lipids in air-dried camel jerky

A non-targeted lipidomics, using UHPLC-Q-Exactive Orbitrap MS/MS in positive and negative ion modes identified 606 lipids from air-dried camel jerky, belonging to 6 main classes. These were glycerophospholipids (GPs) (45.38%), glycerolipids (GLs) (33.17%), sphingolipids (SPs) (13.70%) and the other lipid classes (all<10%) (Fig. 1). The six lipid classes further divided into 30 lipid subclasses, including 25 acylcarnitine (ACar), 1 cholesteryl ester (CE), 14 ceramide non-hydroxyfatty acid-dihydrosphingosine (Cer/NDS), 22 ceramide non-hydroxyfatty acid-sphingosine (Cer/NS), 6 cardiolipin (CL), 1 diacylglycerol (DAG), 11 diacylglyceryl trimethylhomoserine (DGTS), 11 free fatty acid (FA), 3 fatty acid ester of hydroxyl fatty acid (FAHFA), 4

glucuronosyldiacylglycerol (GlcADG), 1 ganglioside (GM3), 4 hexosylceramide alpha-hydroxy fatty acid-phytospingosine (HexCer/AP), 4 hexosylceramide non-hydroxyfatty acid-dihydrosphingosine (HexCer/NDS), 5 hexosylceramide non-hydroxyfatty acid-sphingosine (HexCer/NS), 8 lysophophatidylcholine (LPC), 12 lysophosphatidylethanolamine (LPE), 1 lysophosphatidylinositol (LPI), 2 monogalactosyldiacylglycerol (MGDG), 1 oxidized phosphatidylinositol (OxPI), 150 phosphatidylcholine (PC), 68 phosphatidylethanolamine (PE), 3 phosphatidylethanol (PEtOH), 7 phosphatidylglycerol (PG), 16 phosphatidylinositol (PI), 1 phosphatidylmethanol (PMeOH), 2 phosphatidylserine (PS), 1 sulfurhexosylceramide hydroxyfatty acid (SHexCer), 32 sphingomyelin (SM), 3 sulfoquinovosyl diacylglycerol (SQDG), and 187 triacylglycerol (TAG). TAGs were the most abundant lipid subclasses, followed by PCs and PEs accounting for 30.86%, 24.75% and 11.22% of the total lipid content, respectively.

The lipid content in camel jerky during air-dried processing underwent changes (Fig. 2A), and likewise each lipid subclass (Fig. 2B). Total GL content fluctuated during the drying period; it was high during the curing stage (from raw meat to salted for 3d), which decreased from air-dried 0d to 4d, increased from air-dried 4d to 6d, and decreased from air-dried 6d to 8d. TAG content underwent similar changes as GLs during processing, and DAG content increased with the extension of air-drying time, which may be due to the hydrolysis of TAG. Furthermore, total GP and SP contents increased in salted meat for 3 d after air-drying, compared to raw meat. Most of the lipid subclasses, such as PC, PE, PG, Cer/NS, and CL, increased during the air-drying stage (Fig. 2B). PC and PE are the main components of GP and are the most abundant phospholipids in all mammalian cell membranes, which protect membrane structure and participate in lipid metabolism (van der Veen et al., 2017). Cer is a key neutral lipid, and has two long hydrocarbon chains, which is a sphingolipid decomposition product of biofilm bilayers (Siebers et al., 2016). CL was identified as a key phospholipid of the mitochondrial inner membrane, whereby unsaturated CL acyl chains perform an important role in the integrity and function of the inner mitochondrial membrane (Li et al., 2023). Total fatty acyls content also exhibited an overall increasing trend, and the decomposition of lipids was accompanied by the production of free fatty acids, likely due to their release from glycerolipids (Storrustløkken et al., 2015).

3.2. Fatty acid composition of TAGs, PCs, and PEs in air-dried camel meat

The fatty acid composition of TAGs, PCs and PEs was analyzed to evaluate the proportion of saturated fatty acid (SFA), monounsaturated

Fig. 1. (A) Types of lipid molecules in positive and negative ion modes during air-dried camel jerky processing; (B) Pie plot of lipid classification and proportion.
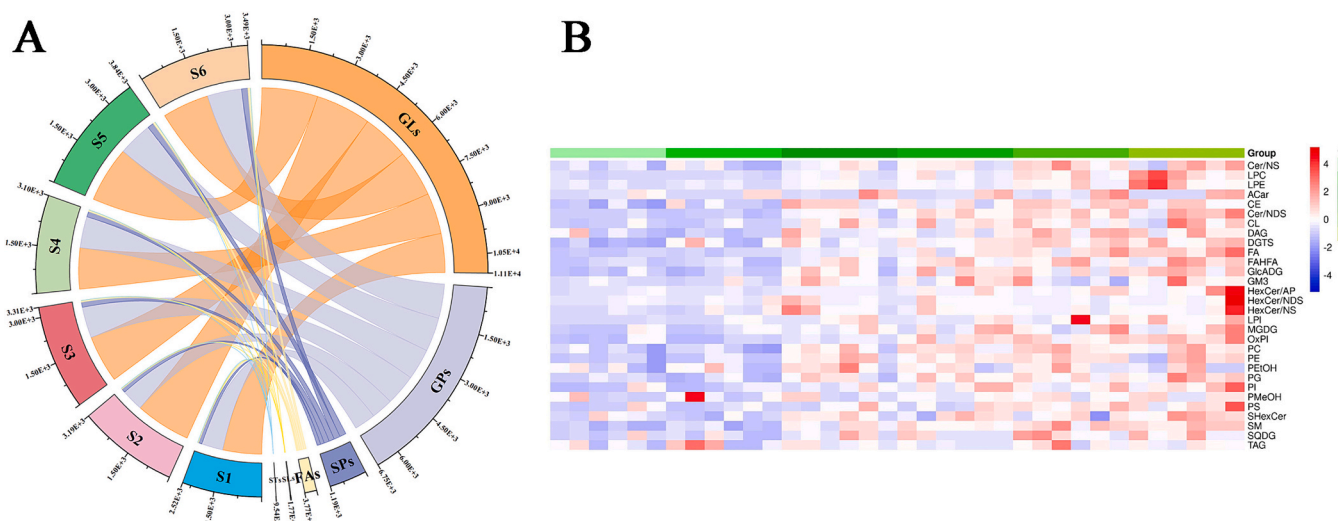
Fig. 2. (A) Dynamic changes in lipid content in air-dried jerky during processing; (B) Cluster heat map of lipids during air-dried camel jerky processing.

fatty acid (MUFA), di-unsaturated fatty acid (DUFA), and poly-unsaturated fatty acid (PUFA) (Fig. 3). SFAs, MUFAs, DUFAs, and PUFAs in camel jerky dried for 8d accounted for 44.50%, 32.62%, 6.21%, and 16.67% of TAGs, respectively. Further analysis of the fatty acid profile revealed that the most abundant SFA, MUFA, DUFA, and PUFA in TAGs were palmitic acid (16:0), oleic acid (18:1), linoleic acid (18:2), and C12:3, respectively. In PCs, the relative SFA, MUFA, DUFA, and PUFA contents were 38.59%, 15.44%, 14.77%, and 31.21%, respectively. The major fatty acids identified in PCs included C14:0e, palmitoleic acid (16:1), linoleic acid (18:2), and docosapentaenoic acid (DPA, 22:5). In PEs, SFAs, MUFAs, DUFAs, and PUFAs accounted for 27.94%, 13.97%, 20.59%, and 37.50%, respectively. Palmitic acid (16:0), oleic acid (18:1), linoleic acid (18:2), and arachidonic acid (20:4) represented the major fatty acids in PEs. Most of the fatty acids were bound to other

complex lipids, and usually only a small portion existed as free fatty acids. Long-chain fatty acids were the largest and most diverse group of fatty acids and were commonly found in animal foods. DPA, linoleic acid and arachidonic acid belonged to the n-3 fatty acids and n-6 fatty acids, which were essential for human nutrition, especially DPA was the direct intermediate between EPA and DHA (Drouin et al., 2019). Wang, Zhong, et al. (2022) found that the relatively high UFA levels in PC and PE accounted for the decrease observed in the overall PC and PE contents during golden pomfret fermentation.

3.3. Differential analysis of lipids during air-dried camel jerky processing

The lipidomic changes in camel jerky at different processing stages were analyzed using an unsupervised PCA model (Fig. 4A). The
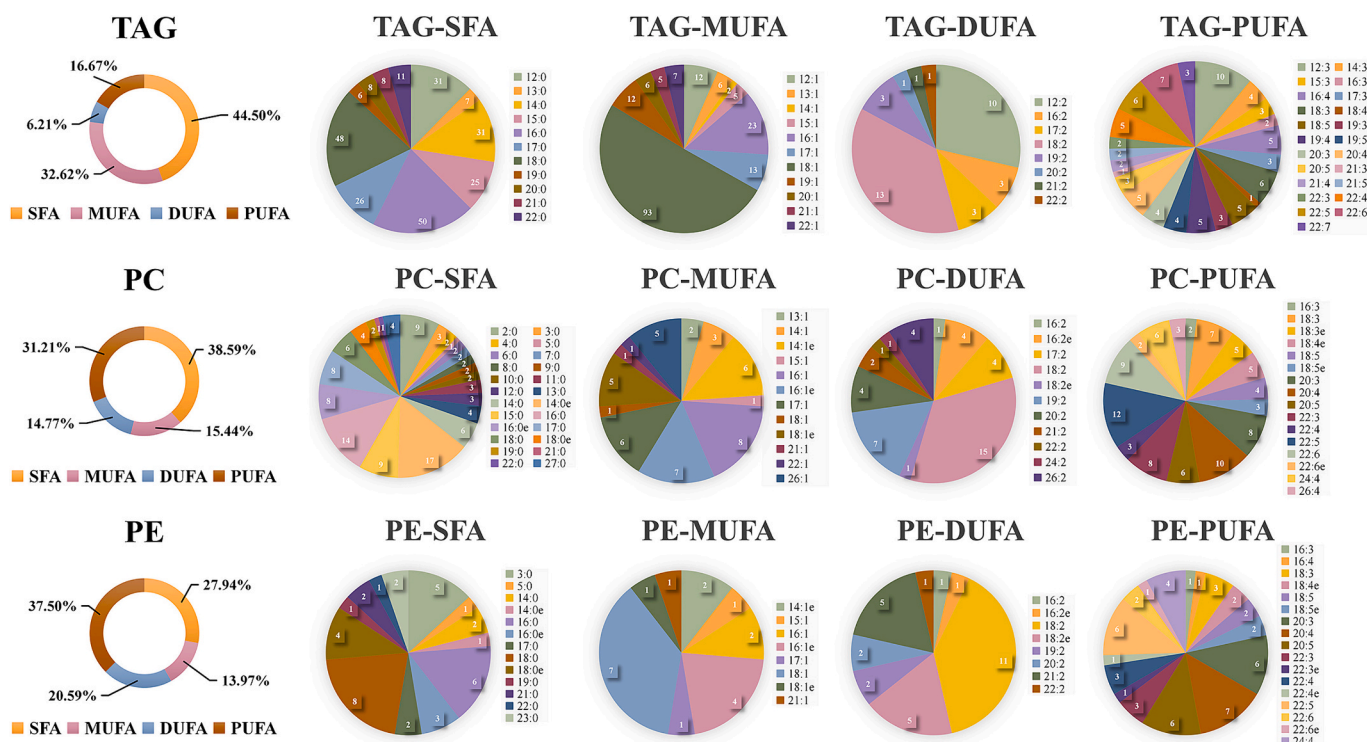
Fig. 3. The fatty acid composition of triglyceride (TAG), phosphatidylcholine (PC) and phosphatidylethanolamine (PE) in air-dried camel meat (air-dried for 8d).
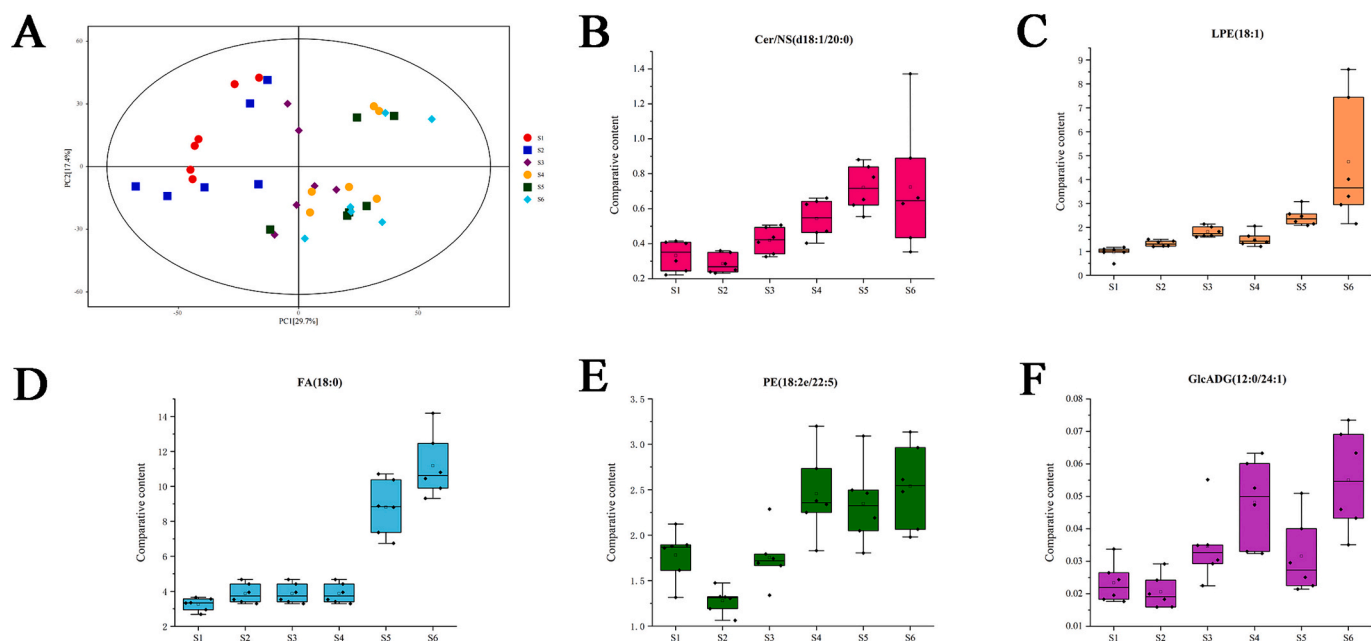
Fig. 4. (A) Scatter plot of principal component analysis scores for all samples; (B—F) Box plots of potential lipid markers revealing the relative content during air-dried camel jerky processing.

contributions of principal components, PC1 and PC2, were 29.7% and 17.4%, respectively. The raw meat and the salted for 3d sample groups were clearly separated from air-dried for 2 d, 4 d, 6 d, and 8 d sample groups, indicating that the lipids were obviously changed during the air-dried stage. The lipids showed a greater degree of change during the early drying stage (air-dried for 2 d), which may have been due to the acceleration of hydrolysis and oxidation of lipids as a result of the loss of water. To discriminate the lipid species among adjacent processing stages of camel jerky, the lipidomic data were analyzed using a supervised OPLS-DA. The OPLS-DA scoring plots showed that each pair of samples for comparison (S2 vs S1, S3 vs S2, S4 vs S3, S5 vs S4, and S6 vs S5) were clearly separated on the left region or on the right region of the

model. The R^2Y values for these five pairs of models were all above 0.9, and the intercepts between the regression line of Q^2 and the y-axis of the five pairs, were <0. This showed that the model did not overfit and was reliable for differential lipid screening. Differential lipids over the adjacent processing stages were screened based on the above-described OPLS-DA model, with VIP > 1 and $P < 0.05$ as the screening criteria. The results showed that a total of 206 differential lipid molecules were screened out in the five pairs samples. Of these, Cer/NS (d18:1/20:0), LPE (18:1), FA (18:0), GlcADG (12:0/24:1), and PE (18:2e/22:5) showed significant differences in three pairs of samples, which contributed significantly to the discrimination of processing stages. The relative content of these five potential lipid markers during camel jerky
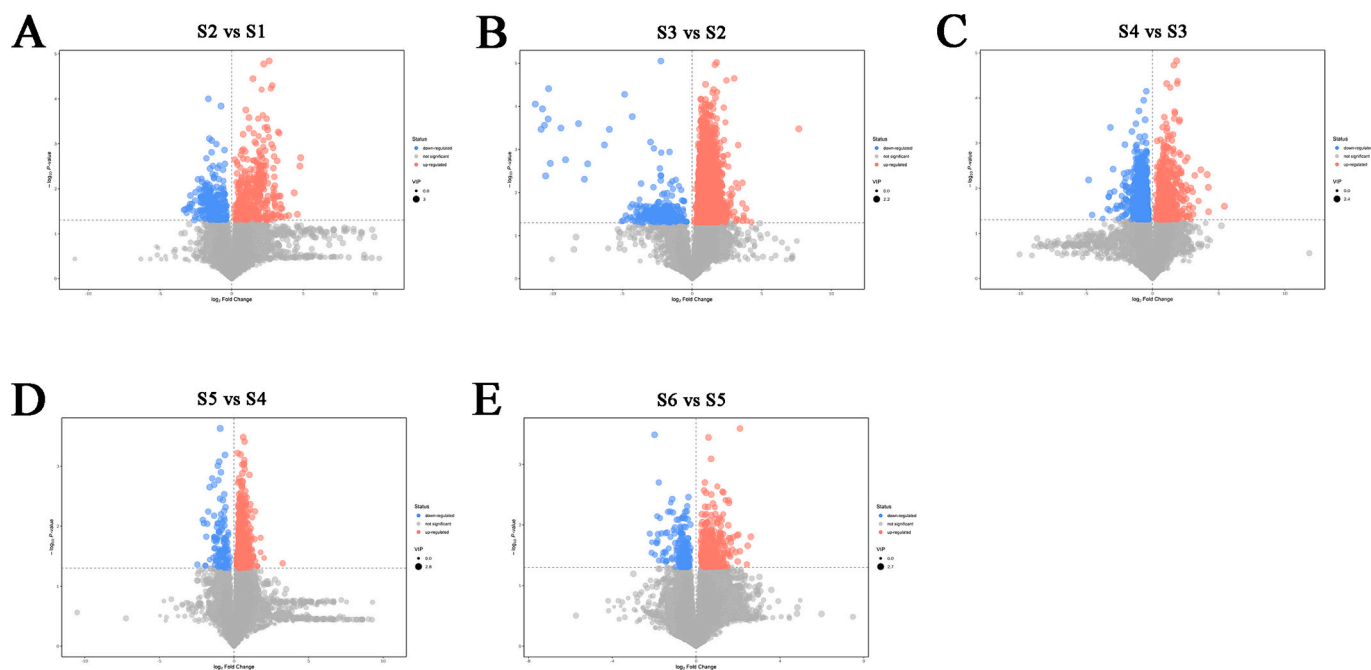

Fig. 5. Volcano plot and matchstick diagram of differential lipid molecules.

processing were presented in Fig. 4B-F. From S1 to S2, LPE (18:1) and FA (18:0) were significant increased ($P < 0.05$), PE (18:2e/22:5) was significant decreased ($P < 0.05$); from S2 to S3, five lipid molecules were significant increased ($P < 0.05$); from S3 to S4, Cer/NS (d18:1/20:0) and PE (18:2e/22:5) were significant increased ($P < 0.05$); from S4 to S5, Cer/NS (d18:1/20:0) and LPE (18:1) were significant increased ($P < 0.05$) and GlcADG (12:0/24:1) was significant decreased ($P < 0.05$); from S5 to S6, FA (18:0) and GlcADG (12:0/24:1) were significant increased ($P < 0.05$).

As shown in the volcano plot (Fig. 5), TAG (12:0/22:6/22:6), DGTS (13:1/18:4), DGTS (16:4/18:5), HexCer/NS (d18:1/24:0), LPE (18:1), DGTS (13:1/20:4), PC (11:0/26:2), TAG (12:0/12:0/22:1), and FA (18:0) were significantly upregulated, and PE (18:2e/22:5), PC (18:3e/17:2), and PC (16:0/15:1) were significantly downregulated from S1 to S2. From raw meat to cured 3d, glycerides represented by TAG and DGTS were significantly upregulated, and the glycerophospholipids containing polyunsaturated fatty acids were significantly downregulated due to the hydrolysis of glycerophospholipids by phospholipase. From S2 to S3, 167 lipids molecules such as TAG (12:0/12:0/17:3), PC (18:5e/19:2), SM (d14:0/19:1), PC (18:4e/15:0), PC (14:0e/16:1), PC (18:4e/19:0), SM (d18:0/18:1), SM (d14:1/28:0), and PC (14:1e/2:0) were upregulated, and Cer/NS (d18:3/30:2) was significantly downregulated, indicating that the lipid molecules changed dramatically from salted for 3d to air-dried for 2d. The significant increase in linoleic acid in air-dried for 0–2 d may have been responsible for the hydrolysis of PC. For example, an increase in linoleic acid FFA (18:1) and FFA (18:2) during the cold storage of Sanhuang chicken was suggested to have been partly due to the hydrolysis of PC (18:2/18:2) and PC (16:0/18:3) (Lv et al., 2023). From S3 to S4, 26 lipids such as TAG (12:2/12:2/22:6), TAG (12:1/16:4/16:4), SQDG (16:0/16:1), PE (16:2e/18:2), PE (14:1e/20:4), and PC (7:0/26:2) were significantly upregulated, and 20 lipids such as PC (22:6e/13:0), PC (20:4/20:4), PC (18:0/18:5), PC (16:1/16:1), and PC (14:1e/19:2) were significantly downregulated. Lipids containing polyunsaturated fatty acids were down-regulated, while glycerophospholipids and sphingolipids containing saturated fatty acids were up-regulated during air-drying for 2d to 4d, indicating that air-dried camel meat may have undergone a certain degree of lipid oxidation. From S4 to S5, 18 lipids such as PS (18:0/18:1), PE (21:2/20:3), PS (18:0/18:2), PC (16:0/20:4), FA (22:4), TAG (16:0/17:0/18:1), and TAG (16:0/16:0/18:0) were significantly upregulated, and GlcADG (12:0/24:1) was significantly downregulated. From S5 to S6, 6 lipids such as LPE (16:0), GlcADG (12:0/24:1), PC (14:1/26:4), SM (d14:0/20:1), and SM (d14:0/20:0) were significantly upregulated, and 3 lipids were significantly downregulated. The downregulated lipids were glycerides containing unsaturated fatty acids during air-drying for 6–8 d. Lipids and free fatty acids of glycolipids were significantly up-regulated, which indicated that lipid hydrolysis was still ongoing in the later stage of air drying. Lipid molecules belonging to TG, PC, PE, LPE, DG, Cer, PS and SQDG were also showed significant differences among the different processing times in Nuodeng ham. Additionally, the content of TG and DG increased, the PC decreased, and PS, PE, LPE were interconverted due to oxidation reactions and enzymatic hydrolysis during Nuodeng ham processing. (Yang et al., 2023). On a whole, TAG, PC and PE fatty acid chains increased during processing of air-dried camel meat, indicating that lipid degradation led to changes in lipid structure. During dry-cured mutton ham processing, levels of PUFA-containing lipids increased, including arachidonic acid, and DPA, besides linoleic acid and α-linolenic acid also showed an upward trend (Guo et al., 2022). Air-drying might promote the degradation of TAG, the conversion of glycerophospholipids to lysophospholipids, the saturation of the unsaturated fatty acid chain of glycerophospholipids, as well as the accumulation of sphingolipids and fatty acids (Wang, Zhong, et al., 2022). From curing to drying, most of the differential lipids in mackerel showed upregulation. The major pathways of lipid metabolism during the dry-cured processing of mackerel were glycerophospholipid metabolism, in which DG, PG,

PE, PC and LPC are mainly involved, and sphingolipid metabolism, which was mediated by SM and Cer (Liu et al., 2023).

3.4. Differential analysis of volatile compounds emitted during air-dried camel jerky processing

A total of 96 volatile compounds were detected by HS-SPME-GC-ToF-MS, including 23 hydrocarbons, 16 alcohols, 15 aldehydes, 13 ketones, 6 acids, 4 esters, 4 lactones, and 15 other compounds such as heterocyclic, phenols, nitrogen-phosphorus etc. (Table 1). The main volatiles in the finished air-dried camel jerky (S6) were acetoin, 1-hexanol, 2-ethyl-, ethanol, heptane, 2,2,4,6,6-pentamethyl-, 1-octen-3-ol, pentanal, butanoic acid, toluene and acetic acid. The total amount of volatile compounds increased in the curing stage and decreased in the air-drying for 0–2 d. The total amount of volatile compounds increased continuously with the extension of air-drying time, and that of finished air-dried camel jerky (S6) was 1.75 times that of raw meat. Aldehyde content increased in the curing stage, decreased in the air-drying for 0–4 d stage, increased in the air-drying for 4–8 d stage, and was higher in finished camel jerky than in raw camel meat. Aldehydes were identified as the most abundant volatile compounds produced during the curing process in some dry-cured meat products (Lorenzo & Carballo, 2015). Also, the inhibitory effect of salt on lipid oxidation was suggested to be due to the aldehyde content in dry-cured pork, which gradually decreased with increase in salt amount (Tian et al., 2020). In this study, alcohol amount increased in the curing stage, decreased in the early air-drying stage, and then increased with the extension of air-drying time. Alcohols are important volatile compounds, which produce the special fat flavor of meat (Zhang et al., 2020). 1-Octen-3-ol, 1-pentanol and 2-ethyl-1-hexanol were alcohols with high levels in stir-fried pork tenderloin, and the increase in 1-octen-3-ol content after cooking may have been due to lipid oxidation (Wang et al., 2023).The volatiles, 2-ethylhexanol and 1-octen-3-ol were emitted during yak jerky processing, which increased with the extension of air-drying time (Han et al., 2020). Linoleic acid degradation produced ethanol which was one of the most abundant volatile compounds in dry-cured meat products. Further, ketone content increased gradually from raw meat to air-dried 6 d, and decreased from air-dried 6 d to 8 d. Acetoin content increased in dry-cured beef with the extension of storage time (Xu et al., 2020). The volatile, 2-butanone was abundant in Jinhua ham, which increased continuously during processing (Li, Geng, et al., 2022). This was consistent with the results of this experiment. Hydrocarbon content increased continuously during the whole processing of air-dried camel jerky, and the degree of change was the largest in the air-dried 2–4 d. Fat oxidation produces hydrocarbons, which were the highest amount of volatile compounds in spiced beef jerky, especially toluene, *p*-xylene, undecane and dodecane (Zhou et al., 2021).

PCA and OPLS-DA were applied to identify the differences in volatile compounds during different processing stages of camel jerky. Samples from adjacent processing periods were used as controls, and the screening conditions were VIP > 1 and $P < 0.05$. A total of 61 differential volatile compounds were screened in the 5 pairs, as shown in the Venn diagram (Fig. 6B). There were significant differences in tridecane, 3-methyl- and tetradecane, 3-methyl- among the five pairs, which could be used as potential biomarkers to distinguish two adjacent processing stages. Tridecane, 3-methyl- content decreased in the curing stage, increased in the air-drying stage, and was the highest in the air-dried camel meat after air-drying for 8 days. Tetradecane, 3-methyl- content increased in the curing stage, decreased in the air-dried 0–2 d, increased in the air-dried 2–6 d, decreased again in the air-dried 6–8 d, and was the highest in the air-dried 6 d. From S1 to S2, 11 differential volatile compounds including benzenemethanol,dimethyl-, acetophenone, 2-decanone, ethyl acetate and 1-dodecanol were significantly upregulated and tridecane, 3-methyl- and 1-tetradecene were significantly down-regulated. From S2 to S3, 15 differential volatile compounds including 3-ethyl-2,6,10-trimethylundecane, decane, 2-

Table 1
Volatile compounds in air-dried camel meat during processing.

Compounds	CAS	Comparative content					
		S1	S2	S3	S4	S5	S6
Aldehydes							
Butanal, 2-methyl-	96–17-3	0.004 ± 0.001 [c]	0.002 ± 0.002 [c]	0.005 ± 0.003 [c]	0.009 ± 0.004 [b]	0.009 ± 0.004 [b]	0.015 ± 0.003 [a]
Butanal, 3-methyl-	590–86-3	0.001 ± 0.000 [c]	0.002 ± 0.002 [bc]	0.002 ± 0.003 [bc]	0.002 ± 0.002 [bc]	0.004 ± 0.002 [b]	0.008 ± 0.003 [a]
Pentanal	110–62-3	0.107 ± 0.070 [c]	0.203 ± 0.124 [bc]	0.198 ± 0.067 [bc]	0.247 ± 0.089 [ab]	0.314 ± 0.049 [ab]	0.325 ± 0.124 [a]
Hexanal	66–25-1	0.384 ± 0.421	0.364 ± 0.440	0.316 ± 0.116	0.096 ± 0.053	0.084 ± 0.040	0.161 ± 0.098
Octanal	124–13-0	0.005 ± 0.012	0.023 ± 0.020	0.008 ± 0.010	0.003 ± 0.002	0.003 ± 0.005	0.000 ± 0.000
Nonanal	124–19-6	0.013 ± 0.013	0.019 ± 0.016	0.018 ± 0.007	0.013 ± 0.008	0.015 ± 0.003	0.030 ± 0.009
Benzaldehyde	100–52-7	0.012 ± 0.009	0.018 ± 0.013	0.015 ± 0.007	0.018 ± 0.006	0.023 ± 0.012	0.038 ± 0.023
2-Nonenal, (E)-	18,829–56-6	0.000 ± 0.000	0.001 ± 0.000	0.000 ± 0.000	0.001 ± 0.001	0.003 ± 0.002	0.003 ± 0.002
Dodecanal	112–54-9	0.001 ± 0.001	0.002 ± 0.001	0.001 ± 0.000	0.002 ± 0.001	0.003 ± 0.002	0.005 ± 0.004
2-Undecenal	53,448–07-0	0.001 ± 0.001	0.001 ± 0.001	0.001 ± 0.000	0.000 ± 0.000	0.000 ± 0.000	0.000 ± 0.000
Tetradecanal	124–25-4	0.003 ± 0.003	0.003 ± 0.003	0.003 ± 0.001	0.002 ± 0.001	0.002 ± 0.001	0.005 ± 0.002
Pentadecanal-	2765-11-9	0.006 ± 0.005	0.011 ± 0.006	0.005 ± 0.002	0.004 ± 0.002	0.010 ± 0.006	0.016 ± 0.009
13-Methyltetradecanal	75,853–51-9	0.001 ± 0.000	0.001 ± 0.000	0.001 ± 0.000	0.001 ± 0.001	0.002 ± 0.001	0.002 ± 0.001
Hexadecanal	629–80-1	0.014 ± 0.008	0.012 ± 0.008	0.011 ± 0.007	0.025 ± 0.013	0.039 ± 0.024	0.032 ± 0.038
Octadecanal	638–66-4	0.002 ± 0.002	0.002 ± 0.002	0.002 ± 0.002	0.003 ± 0.002	0.006 ± 0.004	0.006 ± 0.005
Alcohols							
Ethanol	64–17-5	0.121 ± 0.135	0.063 ± 0.050	0.170 ± 0.030	0.284 ± 0.056	0.468 ± 0.058	0.598 ± 0.177
1-Butanol	71–36-3	0.022 ± 0.010	0.028 ± 0.013	0.037 ± 0.010	0.035 ± 0.028	0.068 ± 0.015	0.074 ± 0.010
1-Penten-3-ol	616–25-1	0.040 ± 0.039	0.069 ± 0.041	0.042 ± 0.009	0.019 ± 0.018	0.034 ± 0.013	0.056 ± 0.008
1-Butanol, 3-methyl-	123–51-3	0.001 ± 0.001 [b]	0.001 ± 0.001 [b]	0.001 ± 0.001 [b]	0.001 ± 0.002 [b]	0.003 ± 0.001 [a]	0.001 ± 0.001 [b]
1-Pentanol	71–41-0	0.446 ± 0.263	0.650 ± 0.171	0.244 ± 0.056	0.102 ± 0.059	0.093 ± 0.033	0.125 ± 0.032
1-Hexanol	111–27-3	0.203 ± 0.123	0.289 ± 0.126	0.073 ± 0.030	0.034 ± 0.039	0.023 ± 0.027	0.043 ± 0.020
1-Octen-3-ol	3391-86-4	0.531 ± 0.401	0.559 ± 0.463	0.402 ± 0.109	0.235 ± 0.138	0.264 ± 0.069	0.423 ± 0.127
1-Heptanol	111–70-6	0.098 ± 0.068	0.117 ± 0.104	0.050 ± 0.028	0.027 ± 0.033	0.023 ± 0.020	0.017 ± 0.026
1-Hexanol, 2-ethyl-	104–76-7	0.675 ± 0.460 [a]	1.045 ± 0.541 [a]	0.625 ± 0.344 [a]	0.951 ± 0.713 [a]	0.946 ± 0.383 [a]	0.960 ± 0.291 [a]
1-Octanol	111–87-5	0.074 ± 0.065	0.114 ± 0.094	0.069 ± 0.033	0.051 ± 0.038	0.052 ± 0.016	0.066 ± 0.006
1-Nonanol	143–08-8	0.003 ± 0.002	0.005 ± 0.005	0.001 ± 0.001	0.000 ± 0.000	0.000 ± 0.000	0.000 ± 0.000
1-Heptanol, 2-propyl-	10,042–59-8	0.002 ± 0.002	0.070 ± 0.037	0.070 ± 0.031	0.103 ± 0.056	0.078 ± 0.023	0.069 ± 0.012
Benzenemethanol,dimethyl-	13,651–14-4	0.000 ± 0.000	0.071 ± 0.011	0.066 ± 0.018	0.104 ± 0.042	0.110 ± 0.019	0.122 ± 0.013
trans-2-Dodecen-1-ol	69,064–37-5	0.002 ± 0.002	0.001 ± 0.002	0.002 ± 0.001	0.001 ± 0.001	0.002 ± 0.001	0.004 ± 0.001
Benzyl alcohol	100–51-6	0.001 ± 0.001	0.002 ± 0.001	0.016 ± 0.005	0.030 ± 0.009	0.040 ± 0.007	0.051 ± 0.010
1-Dodecanol	112–53-8	0.001 ± 0.001 [c]	0.003 ± 0.001 [b]	0.003 ± 0.001 [b]	0.004 ± 0.001 [b]	0.006 ± 0.001 [a]	0.006 ± 0.001 [a]
Ketones							
2-Butanone	78–93-3	0.014 ± 0.010 [c]	0.013 ± 0.005 [c]	0.010 ± 0.002 [c]	0.016 ± 0.003 [c]	0.025 ± 0.005 [b]	0.033 ± 0.005 [a]
2,3-Pentanedione	600–14-6	0.016 ± 0.018	0.013 ± 0.022	0.012 ± 0.003	0.003 ± 0.003	0.006 ± 0.004	0.006 ± 0.003
3-Heptanone	106–35-4	0.002 ± 0.001	0.017 ± 0.003	0.007 ± 0.002	0.010 ± 0.004	0.013 ± 0.002	0.017 ± 0.001
2-Heptanone, 6-methyl-	928–68-7	0.010 ± 0.007	0.012 ± 0.011	0.006 ± 0.003	0.004 ± 0.003	0.004 ± 0.001	0.005 ± 0.001
3-Octanone	106–68-3	0.001 ± 0.000	0.001 ± 0.001	0.001 ± 0.000	0.001 ± 0.001	0.001 ± 0.001	0.002 ± 0.001
Acetoin	513–86-0	1.086 ± 0.751	1.138 ± 0.759 [c]	1.561 ± 0.589 [bc]	2.164 ± 0.547 [ab]	2.529 ± 0.381 [a]	2.437 ± 0.747 [a]
5-Hepten-2-one, 6-methyl-	110–93-0	0.005 ± 0.003 [c]	0.005 ± 0.004 [c]	0.006 ± 0.001 [bc]	0.009 ± 0.003 [abc]	0.010 ± 0.001 [bc]	0.010 ± 0.005 [a]
2-Pentanone, 4-hydroxy-4-methyl-	123–42-2	0.002 ± 0.002	0.005 ± 0.000	0.012 ± 0.004	0.013 ± 0.003	0.019 ± 0.006	0.024 ± 0.008
2-Nonanone	821–55-6	0.004 ± 0.004 [a]	0.006 ± 0.007 [a]	0.003 ± 0.002 [a]	0.005 ± 0.005 [a]	0.007 ± 0.004 [a]	0.007 ± 0.007 [a]
2,3-Nonanedione	57,644–90-3	0.000 ± 0.000	0.001 ± 0.001	0.000 ± 0.000	0.001 ± 0.000	0.001 ± 0.001	0.002 ± 0.001
2-Decanone	693–54-9	0.003 ± 0.001	0.006 ± 0.002	0.003 ± 0.002	0.004 ± 0.001	0.005 ± 0.001	0.007 ± 0.004
Acetophenone	98–86-2	0.006 ± 0.004	0.039 ± 0.008	0.054 ± 0.018	0.090 ± 0.037	0.110 ± 0.025	0.131 ± 0.023
5,9-Undecadien-2-one, 6,10-dimethyl-, (E)-	3796-70-1	0.006 ± 0.002 [b]	0.006 ± 0.002 [b]	0.006 ± 0.002 [b]	0.008 ± 0.002 [ab]	0.010 ± 0.001 [a]	0.009 ± 0.005 [ab]
Acids							
Acetic acid	64–19-7	0.019 ± 0.024	0.026 ± 0.031	0.104 ± 0.058	0.087 ± 0.081	0.305 ± 0.094	0.201 ± 0.074
Butanoic acid	107–92-6	0.163 ± 0.185 [a]	0.335 ± 0.266 [a]	0.346 ± 0.319 [a]	0.259 ± 0.363 [a]	0.214 ± 0.275 [a]	0.295 ± 0.209 [a]
Hexanoic acid	142–62-1	0.309 ± 0.246	0.341 ± 0.384	0.176 ± 0.184	0.139 ± 0.228	0.268 ± 0.416	0.042 ± 0.103
Hexanoic acid, 2-ethyl-	149–57-5	0.017 ± 0.017	0.056 ± 0.026	0.041 ± 0.017	0.065 ± 0.027	0.041 ± 0.021	0.070 ± 0.070
Dodecanoic acid	143–07-7	0.003 ± 0.003	0.004 ± 0.002	0.002 ± 0.002	0.005 ± 0.005	0.009 ± 0.008	0.003 ± 0.003
Tetradecanoic acid	544–63-8	0.003 ± 0.003 [bc]	0.001 ± 0.001 [c]	0.002 ± 0.002 [c]	0.004 ± 0.002 [bc]	0.006 ± 0.003 [ab]	0.009 ± 0.004 [a]
Esters							

Table 1 (*continued*)

Compounds	CAS	Comparative content					
		S1	S2	S3	S4	S5	S6
Acetic acid, methyl ester	79–20-9	0.004 ± 0.001	0.003 ± 0.002	0.005 ± 0.002	0.009 ± 0.011	0.014 ± 0.012	0.021 ± 0.017
Ethyl Acetate	141–78-6	0.000 ± 0.000	0.008 ± 0.006	0.007 ± 0.001	0.010 ± 0.003	0.011 ± 0.002	0.013 ± 0.003
Butanoic acid, ethyl ester	105–54-4	0.001 ± 0.001 [c]	0.000 ± 0.001 [c]	0.002 ± 0.001 [bc]	0.003 ± 0.002 [b]	0.006 ± 0.001 [a]	0.008 ± 0.004 [a]
n-Caproic acid vinyl ester	3050-69-9	0.018 ± 0.017	0.001 ± 0.002	0.021 ± 0.016	0.012 ± 0.004	0.015 ± 0.007	0.034 ± 0.021
Lactones							
Butyrolactone	96–48-0	0.030 ± 0.005	0.038 ± 0.013	0.034 ± 0.011	0.061 ± 0.029	0.073 ± 0.018	0.084 ± 0.029
2(3H)-Furanone, 5-ethyldihydro-	695–06-7	0.002 ± 0.002	0.005 ± 0.001	0.003 ± 0.001	0.004 ± 0.002	0.005 ± 0.001	0.006 ± 0.003
2H-Pyran-2-one, tetrahydro-6-methyl-	823–22-3	0.003 ± 0.002	0.003 ± 0.001	0.004 ± 0.002	0.010 ± 0.004	0.016 ± 0.005	0.012 ± 0.011
2(3H)-Furanone, dihydro-5-pentyl-	104–61-0	0.005 ± 0.003	0.007 ± 0.006	0.004 ± 0.003	0.004 ± 0.003	0.004 ± 0.002	0.006 ± 0.002
Hydrocarbons							
Heptane	142–82-5	0.058 ± 0.025 ab	0.047 ± 0.034 ab	0.029 ± 0.014 [b]	0.032 ± 0.020 [b]	0.085 ± 0.053 [a]	0.088 ± 0.048 [a]
Heptane, 2,2,4,6,6-pentamethyl-	13,475–82-6	0.018 ± 0.008	0.021 ± 0.009	0.061 ± 0.028	0.181 ± 0.108	0.240 ± 0.051	0.488 ± 0.124
Decane	124–18-5	0.003 ± 0.001	0.003 ± 0.001	0.010 ± 0.003	0.020 ± 0.006	0.038 ± 0.005	0.056 ± 0.007
Bicyclo[3.1.1]hept-2-ene, 3,6,6-trimethyl-	4889-83-2	0.038 ± 0.051	0.056 ± 0.082	0.082 ± 0.115	0.131 ± 0.181	0.152 ± 0.199	0.161 ± 0.203
Toluene	108–88-3	0.035 ± 0.007	0.041 ± 0.008	0.062 ± 0.017	0.226 ± 0.069	0.217 ± 0.036	0.239 ± 0.031
1-Undecene	821–95-4	0.001 ± 0.001 [c]	0.002 ± 0.001 bc	0.001 ± 0.000 [c]	0.001 ± 0.001 [c]	0.002 ± 0.001 [b]	0.004 ± 0.000 [a]
Undecane	1120-21-4	0.000 ± 0.000	0.000 ± 0.000	0.000 ± 0.000	0.001 ± 0.000	0.002 ± 0.000	0.003 ± 0.002
Ethylbenzene	100–41-4	0.007 ± 0.002 [d]	0.010 ± 0.004 [d]	0.013 ± 0.008 [d]	0.024 ± 0.007 [c]	0.034 ± 0.006 [b]	0.046 ± 0.005 [a]
o-Xylene	95–47-6	0.000 ± 0.000 [c]	0.001 ± 0.001 [c]	0.001 ± 0.001 [c]	0.002 ± 0.000 [b]	0.002 ± 0.001 [b]	0.004 ± 0.000 [a]
p-Xylene	106–42-3	0.006 ± 0.005 [d]	0.009 ± 0.004 cd	0.011 ± 0.006 [c]	0.019 ± 0.006 [b]	0.024 ± 0.002 [b]	0.030 ± 0.001 [a]
Dodecane	112–40-3	0.007 ± 0.002	0.007 ± 0.004	0.008 ± 0.002	0.010 ± 0.008	0.024 ± 0.002	0.031 ± 0.005
Styrene	100–42-5	0.004 ± 0.005 [e]	0.008 ± 0.009 [e]	0.024 ± 0.013 [d]	0.051 ± 0.011 [c]	0.061 ± 0.007 [b]	0.077 ± 0.003 [a]
Tridecane	629–50-5	0.010 ± 0.001	0.010 ± 0.003	0.012 ± 0.004	0.021 ± 0.004	0.035 ± 0.008	0.052 ± 0.008
Tridecane, 6-methyl-	13,287–21-3	0.001 ± 0.000	0.001 ± 0.001	0.001 ± 0.000	0.003 ± 0.001	0.005 ± 0.003	0.004 ± 0.004
Tridecane, 3-methyl-	6418-41-3	0.001 ± 0.000	0.000 ± 0.000	0.001 ± 0.000	0.002 ± 0.001	0.004 ± 0.001	0.006 ± 0.001
Tetradecane	629–59-4	0.003 ± 0.001	0.003 ± 0.001	0.004 ± 0.002	0.017 ± 0.005	0.030 ± 0.013	0.026 ± 0.024
3-Ethyl-2,6,10-trimethylundecane		0.005 ± 0.003	0.002 ± 0.001	0.007 ± 0.002	0.027 ± 0.012	0.044 ± 0.015	0.059 ± 0.015
1-Tetradecene	1120-36-1	0.000 ± 0.000	0.000 ± 0.000	0.000 ± 0.000	0.000 ± 0.000	0.000 ± 0.000	0.000 ± 0.000
Tetradecane, 3-methyl-	18,435–22-8	0.004 ± 0.001	0.006 ± 0.002	0.003 ± 0.001	0.006 ± 0.002	0.011 ± 0.004	0.004 ± 0.006
Hexadecane	544–76-3	0.006 ± 0.001	0.005 ± 0.001	0.008 ± 0.003	0.036 ± 0.013	0.070 ± 0.033	0.042 ± 0.055
Heptadecane	629–78-7	0.001 ± 0.000	0.002 ± 0.001	0.002 ± 0.001	0.013 ± 0.005	0.024 ± 0.012	0.025 ± 0.026
Octadecane	593–45-3	0.001 ± 0.000	0.002 ± 0.001	0.005 ± 0.001	0.011 ± 0.002	0.017 ± 0.003	0.025 ± 0.005
3,7,11,15-Tetramethylhexadec-2-ene		0.002 ± 0.001 [d]	0.002 ± 0.002 cd	0.003 ± 0.001 bcd	0.004 ± 0.002 abc	0.005 ± 0.003 ab	0.006 ± 0.002 [a]
Others							
Furan, 2-ethyl-	3208-16-0	0.015 ± 0.023	0.019 ± 0.024	0.014 ± 0.010	0.004 ± 0.003	0.005 ± 0.005	0.009 ± 0.007
2-n-Butyl furan	4466-24-4	0.004 ± 0.003 [a]	0.008 ± 0.006 [a]	0.006 ± 0.003 [a]	0.004 ± 0.002 [a]	0.006 ± 0.004 [a]	0.004 ± 0.005 [a]
Furan, 2-pentyl-	3777-69-3	0.092 ± 0.066	0.091 ± 0.089	0.091 ± 0.037	0.039 ± 0.022	0.039 ± 0.017	0.087 ± 0.073
Dimethyl sulfide	75–18-3	0.001 ± 0.001	0.002 ± 0.002	0.002 ± 0.001	0.004 ± 0.002	0.006 ± 0.004	0.005 ± 0.004
Dimethyl sulfone	67–71-0	0.014 ± 0.006	0.015 ± 0.008	0.020 ± 0.010	0.040 ± 0.019	0.064 ± 0.027	0.084 ± 0.017
Triisobutyl phosphate	126–71-6	0.005 ± 0.001	0.004 ± 0.003	0.005 ± 0.002	0.007 ± 0.002	0.016 ± 0.005	0.022 ± 0.011
Phenol	108–95-2	0.001 ± 0.000 [e]	0.001 ± 0.001 [e]	0.003 ± 0.001 [d]	0.005 ± 0.001 [c]	0.007 ± 0.001 [b]	0.009 ± 0.001 [a]
Niacinamide	98–92-0	0.001 ± 0.001 [c]	0.001 ± 0.001 [c]	0.001 ± 0.001 [c]	0.003 ± 0.002 [b]	0.004 ± 0.001 ab	0.005 ± 0.001 [a]
unknown		0.008 ± 0.005 [d]	0.012 ± 0.008 [d]	0.017 ± 0.009 cd	0.025 ± 0.010 [c]	0.039 ± 0.005 [b]	0.052 ± 0.004 [a]
unknown		0.003 ± 0.005 [b]	0.003 ± 0.005 [b]	0.001 ± 0.003 [b]	0.001 ± 0.002 [b]	0.002 ± 0.002 [b]	0.009 ± 0.004 [a]
unknown		0.002 ± 0.002	0.001 ± 0.002	0.002 ± 0.001	0.001 ± 0.001	0.002 ± 0.001	0.003 ± 0.001
unknown		0.000 ± 0.000	0.000 ± 0.000	0.000 ± 0.000	0.001 ± 0.001	0.004 ± 0.002	0.005 ± 0.004
unknown		0.008 ± 0.006	0.006 ± 0.009	0.007 ± 0.002	0.005 ± 0.004	0.005 ± 0.004	0.010 ± 0.005
unknown		0.001 ± 0.000	0.000 ± 0.000	0.000 ± 0.000	0.001 ± 0.001	0.002 ± 0.001	0.002 ± 0.002
unknown		0.001 ± 0.001	0.002 ± 0.001	0.001 ± 0.001	0.001 ± 0.001	0.002 ± 0.001	0.003 ± 0.002

pentanone, 4-hydroxy-4-methyl-, octadecane and heptane, 2,2,4,6,6-pentamethyl- were significantly up-regulated, and 7 differential volatile compounds were significantly down-regulated, including 3-heptanone, 1-hexanol, 1-pentanol, tetradecane, 3-methyl- and 2-decanone. From S3 to S4, 24 differential volatile compounds including heptadecane, hexadecane, tetradecane, toluene and octadecane were upregulated, and 7 differential volatile compounds such as hexanal, 1-pentanol, furan, 2-pentyl-, 1-octen-3-ol and furan, 2-ethyl- were downregulated. From S4 to S5, 17 differential volatile compounds including triisobutyl phosphate, tridecane, 3-methyl-, octadecane, ethanol and undecane were significantly upregulated. From S5 to S6, 24 differential volatile compounds including 1-undecene, p-xylene, decane, styrene and heptane, 2,2,4,6,6-pentamethyl- were significantly up-regulated, and tetradecane, 3-methyl- and 1-butanol, 3-methyl- were down-regulated.

Differential volatile compounds during the processing of air-dried camel jerky were mainly dominated by hydrocarbons, alcohols, aldehydes, esters and ketones. The main differential volatile compounds during Dongpo pork dish processing were also categorized as aldehydes,
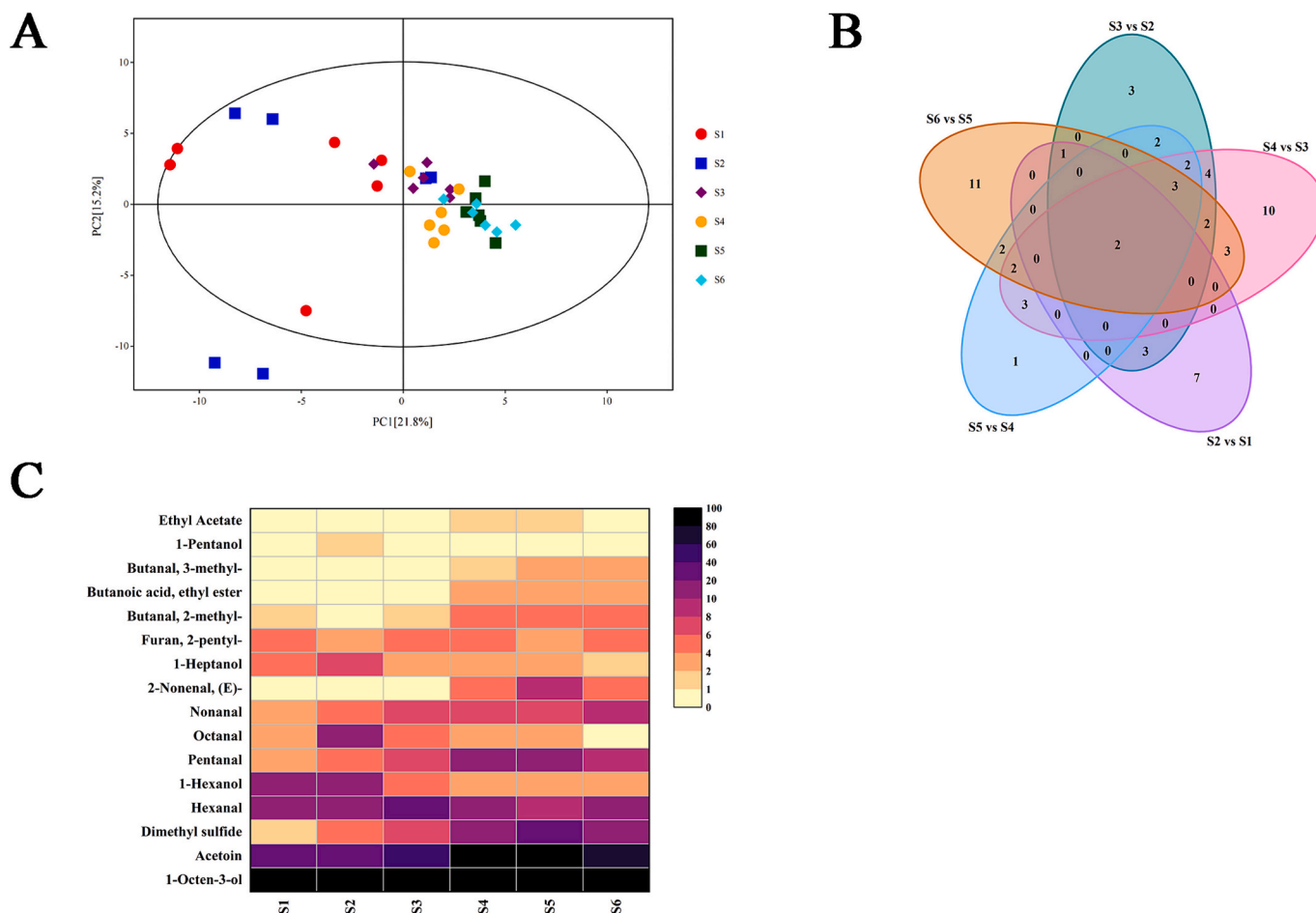
Fig. 6. (A) Score plot of principal component analysis for all samples; (B) Venn diagram of volatile flavor compounds in the processing of air-dried camel jerky; (C) ROAV values of key aroma compounds in air-dried camel jerky during processing.

esters and hydrocarbons (Li, Zheng, et al., 2022). According to the fold change (FC) value of differential volatile compounds, alcohols, esters, and ketones represented by benzenemethanol, dimethyl-, ethyl acetate, 1-heptanol, 2-propyl-, 3-heptanone and acetophenone increased rapidly during the curing stage. And n-caproic acid vinyl ester, benzyl alcohol, acetic acid, butanoic acid and ethyl ester had large increase, and 1-hexanol had a large decrease in the early stage of air-drying. Changes in volatile compounds during the mid-air-drying stage (air-dried 2–6 d) were mainly reflected by the increase of the content of differential hydrocarbons, ketones and esters. In addition, the content of unsaturated aldehydes (2-Nonenal, (*E*)-) and partial long-chain aldehyde increased, while the content of furans decreased during air-dried 2–4 d. Unsaturated aldehydes were widely recognized as one of the most important sources of ham flavor, derived from the degradation of long-chain fatty acids (Liu et al., 2014). In particular, acetic acid was the differential volatile compound which had the maximum increase during air-dried 4–6 d. Acetic acid, which generally originated from auto-oxidation and microbial decomposition, had high odor threshold, and changes in its content might not have much effect on flavor development (Deng et al., 2021). During air-dried 6–8 d, changes of volatile compounds were mainly reflected by the increase of differential aldehydes, alcohols and ketones.

3.5. Identification of key aroma compounds

Human perception of odor is attributed to the sensory threshold and material concentration. ROAV was used to evaluate the odor of air-dried camel meat by combining the sensory threshold with the concentration,

and the ROAV of the volatile compounds that contributed the most to the overall flavor of the sample was defined as 100. The higher the ROAV of volatile compounds, the greater their contribution to the flavor of air-dried camel meat, Compounds with ROAV≥1 were designated as key aroma compounds and 16 volatile compounds with ROAV≥1 were identified during the processing of air-dried camel meat (Fig. 6C), including 1-octen-3-ol (ROAV: 94.98–100), acetoin (ROAV: 22.55–100), dimethyl sulfide (ROV: 1.61–26.05), hexanal (ROAV: 1.34–23.91), 1-hexanol (2.24–17.68), pentanal (ROAV: 2.89–14.46), octanal (ROAV: 0.003–11.42), nonanal (ROAV: 2.89–9.83), 2-nonenal,(E) (ROAV: 0.43–8.08), 1-heptanol (ROAV: 1.13–6.48), furan, 2-pentyl- (ROAV: 3.76–5.76), butanal, 2-methyl- (ROAV: 0.56–5.65), butanoic acid, ethyl ester (ROAV: 0.1903.45), butanal, 3-methyl- (ROAV: 0.38–2.64), 1-pentanol (ROAV: 0.30–1.39) and ethyl acetate (ROAV: 0.0003–1.25). Aldehydes and unsaturated alcohols with low molecular carbon chain greatly contributed to the overall flavor of air-dried camel jerky. Most of these substances had low sensory threshold and were perceived at low concentrations, showing different flavor characteristics such as grass flavor, mushroom flavor, fermentation flavor, oil flavor and fruit flavor. Sulfur compounds with low odor threshold produced the flavor of dried mushrooms, which was one of the important flavors of dry-cured meat (Li, Zhou, et al., 2022). These volatile compounds have been considered as key aroma compounds in other meat products. 1-Octen-3-ol, ethyl acetate, 1-hexanol, nonanal and hexanal were identified as key aroma compounds of donkey, bovine and sheep meat (Man et al., 2023). Also, octanal, nonanal, and 1-octen-3-ol were identified as key aroma compounds in Beijing roast duck (Liu et al., 2019).
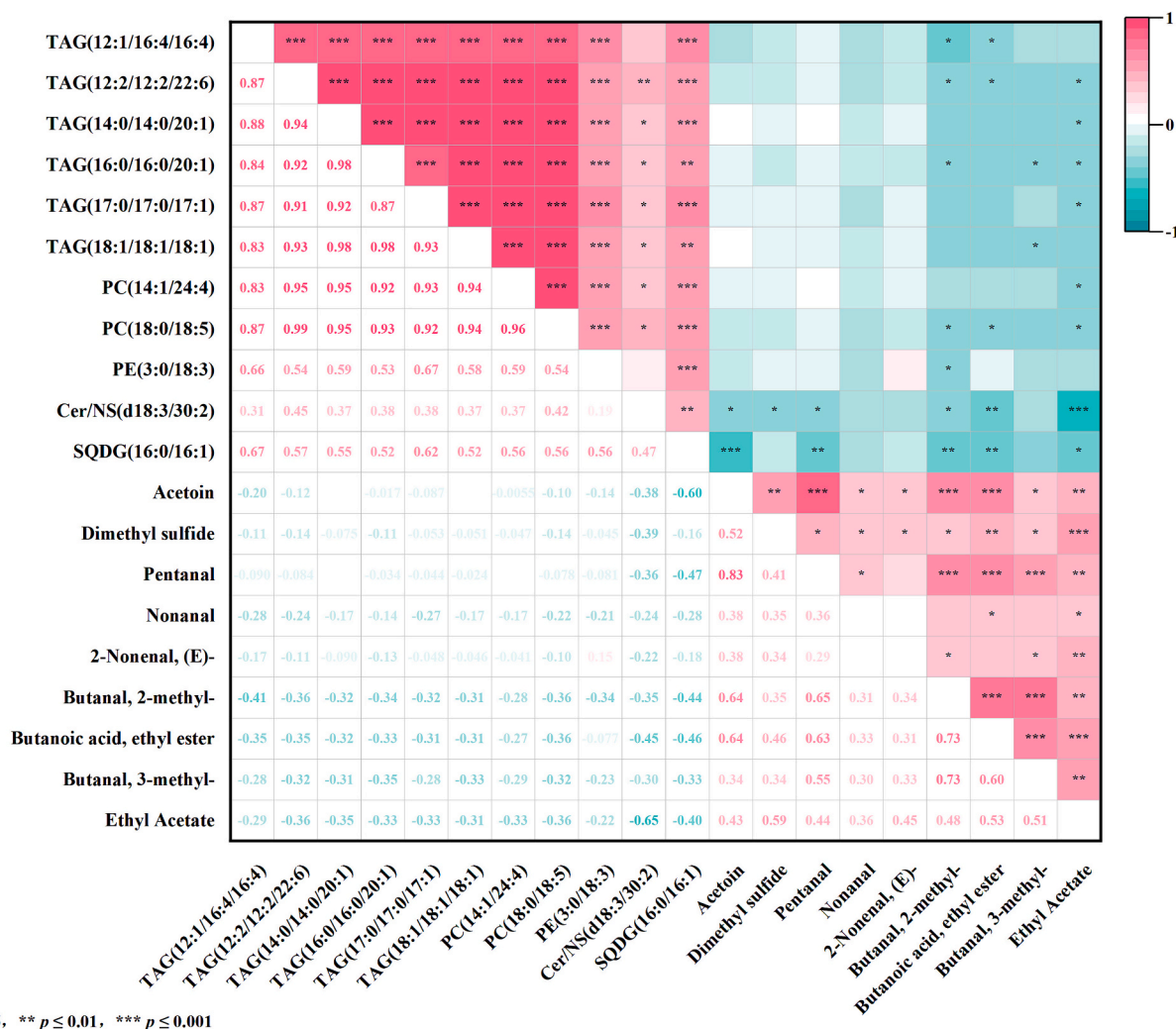
3.6. The relationship between lipids and flavor compounds

Correlation analysis was carried out between 206 differential lipids and 9 key aroma compounds with ROAV≥1, which increased during air-drying for 8d. There was a significant negative correlation between 11 lipids and 7 key aroma compounds during the processing of air-dried camel jerky (*P*< 0.05) (Fig. 7). Cer/NS (d18:3/30:2), SQDG (16:0/16:1), TAG (12:2/12:2/22:6), TAG (16:0/16:0/20:1), and PC (18:0/18:5) significantly negatively correlated with 6, 6, 3, 3 and 3 key aroma compounds respectively. Ethyl acetate significantly negatively correlated (*P*< 0.05) with TAG (12:2/12:2/22:6), TAG (14:0/14:0/20:1), TAG (16:0/16:0/20:1), TAG (17:0/17:0/17:1), PC (14:1/24:4), PC (18:0/18:5), Cer/NS (d18:3/30:2), and SQDG (16:0/16:1). Butanal, 2-methyl- significantly negatively correlated (*P*< 0.05) with TAG (12:1/16:4/16:4), TAG (12:2/12:2/22:6), TAG (16:0/16:0/20:1), PC (18:0/18:5), PE (3:0/18:3), Cer/NS (d18:3/30:2), and SQDG (16:0/16:1). Butanoic acid, ethyl ester significantly negatively correlated (*P*< 0.05) with TAG (12:1/16:4/16:4), TAG (12:2/12:2/22:6), PC (18:0/18:5), Cer/NS (d18:3/30:2), and SQDG (16:0/16:1). Most of these lipids were glycerolipids and the results indicated that the degradation of tri-glycerides and phospholipids containing unsaturated bonds mainly occurred, and probably contributed to the formation of the main aroma compounds during air-dried camel meat processing. Straight chain aliphatic aldehydes such as hexanal, pentanal, octanal and nonanal were produced by unsaturated fatty acids, especially oleic and linoleic acids by autoxidation (Narváez-Rivas et al., 2014). Alcohols are considered the main products of lipid degradation. Linoleic acid was also degraded by lipoxygenase into trans-11-octadecadienoic acid, which was oxidized to 1-octen-3-ol with a strong mushroom flavor to produce meat flavor (Zhang et al., 2018). A high amount of hydrocarbons in foal meat was suggested to have been related to a high C18:1n-9 content (Cittadini et al., 2021).

4. Conclusions

In the study, UHPLC-Q-Exactive Orbitrap MS/MS based non-targeted lipidomics was used to analyze the changes in lipids, and HS-SPME-GC-ToF-MS was used to analyze volatile compounds, during air-dried camel jerky processing. A total of 606 lipid molecules belonging to 30 sub-classes were identified, and a total of 206 differential lipid molecules were screened out. Cer/NS (d18:1/20:0), LPE (18:1), FA (18:0), GlcADG (12:0/24:1), and PE (18:2e/22:5) were identified as potential lipid biomarkers. Moreover, a total of 96 volatile compounds were identified, which included aldehydes, alcohols, esters and hydrocarbons. During air-dried camel meat processing, 61 differential volatile compounds were screened and 16 of these including 1-octen-3-ol, acetoin, dimethyl sulfide, hexanal, 1-hexanol, pentanal, octanal, nonanal, 2-nonenal,(*E*)-, 1-heptanol, furan, 2-pentyl-, butanal, 2-methyl-, butanoic acid, ethyl ester, butanal, 3-methyl-, 1-pentanol and ethyl acetate were identified as key aroma compounds of air-dried camel meat. Eleven differential lipids

	TAG(12:1/16:4/16:4)	TAG(12:2/12:2/22:6)	TAG(14:0/14:0/20:1)	TAG(16:0/16:0/20:1)	TAG(17:0/17:0/17:1)	TAG(18:1/18:1/18:1)	PC(14:1/24:4)	PC(18:0/18:5)	PE(3:0/18:3)	Cer/NS(d18:3/30:2)	SQDG(16:0/16:1)	Acetoin	Dimethyl sulfide	Pentanal	Nonanal	2-Nonenal, (E)-	Butanal, 2-methyl-	Butanoic acid, ethyl ester	Butanal, 3-methyl-	Ethyl Acetate
TAG(12:1/16:4/16:4)		***	***	***	***	***	***	***	***		***						*	*		
TAG(12:2/12:2/22:6)	0.87		***	***	***	***	***	***	***	**	***						*	*		*
TAG(14:0/14:0/20:1)	0.88	0.94		***	***	***	***	***	***	*	***									*
TAG(16:0/16:0/20:1)	0.84	0.92	0.98		***	***	***	***	***	*	**						*		*	*
TAG(17:0/17:0/17:1)	0.87	0.91	0.92	0.87		***	***	***	***	*	***									
TAG(18:1/18:1/18:1)	0.83	0.93	0.98	0.98	0.93		***	***	***	*	**							*		
PC(14:1/24:4)	0.83	0.95	0.95	0.92	0.93	0.94		***	***	*	***									*
PC(18:0/18:5)	0.87	0.99	0.95	0.93	0.92	0.94	0.96		***	*	***						*	*		*
PE(3:0/18:3)	0.66	0.54	0.59	0.53	0.67	0.58	0.59	0.54		***							*			
Cer/NS(d18:3/30:2)	0.31	0.45	0.37	0.38	0.38	0.37	0.37	0.42	0.19		**	*	*	*			*	**		***
SQDG(16:0/16:1)	0.67	0.57	0.55	0.52	0.62	0.52	0.56	0.56	0.56	0.47		***		**			**	**		*
Acetoin	-0.20	-0.12		-0.017	-0.087		-0.10	-0.14	-0.38	-0.60			**	***	*	*	***	***	*	**
Dimethyl sulfide	-0.11	-0.14	-0.075	-0.11	-0.053	-0.051	-0.047	-0.14	-0.045	-0.39	-0.16	0.52			*	*	**			***
Pentanal	0.090	-0.084		-0.034	-0.044	-0.024		-0.078	-0.081	-0.36	-0.47	0.83	0.41		*		***	***	***	**
Nonanal	-0.28	-0.24	-0.17	-0.14	-0.27	-0.17	-0.17	-0.22	-0.21	-0.24	-0.28	0.38	0.35	0.36				*		*
2-Nonenal, (E)-	-0.17	-0.11	-0.090	-0.13	-0.048	-0.046	-0.041	-0.10	0.15	-0.22	-0.18	0.38	0.34	0.29			*		*	**
Butanal, 2-methyl-	-0.41	-0.36	-0.32	-0.34	-0.32	-0.31	-0.28	-0.36	-0.34	-0.35	-0.44	0.64	0.35	0.65	0.31	0.34		***	***	**
Butanoic acid, ethyl ester	-0.35	-0.35	-0.32	-0.33	-0.31	-0.31	-0.27	-0.36	-0.077	-0.45	-0.46	0.64	0.46	0.63	0.33	0.31	0.73		***	***
Butanal, 3-methyl-	-0.28	-0.32	-0.31	-0.35	-0.28	-0.33	-0.29	-0.32	-0.23	-0.30	-0.33	0.34	0.34	0.55	0.30	0.33	0.73	0.60		**
Ethyl Acetate	-0.29	-0.36	-0.35	-0.33	-0.33	-0.31	-0.33	-0.36	-0.22	-0.65	-0.40	0.43	0.59	0.44	0.36	0.45	0.48	0.53	0.51	

* *p* ≤ 0.05，** *p* ≤ 0.01，*** *p* ≤ 0.001

Fig. 7. Correlation between differential lipids and key aroma compounds during air-dried camel jerky processing.

significantly negatively correlated with 7 key aroma compounds during air-dried camel jerky processing ($P < 0.05$). This indicated that the precursors produced by the degradation of lipid molecules were important sources of volatile flavor substances, which contributed to the flavor formation in air-dried camel jerky.

CRediT authorship contribution statement

Shenyi Cao: Writing – review & editing, Writing – original draft, Visualization, Validation, Methodology, Formal analysis, Data curation. **Yinghua Fu:** Writing – review & editing, Supervision, Resources, Project administration, Conceptualization.

Declaration of competing interest

The authors declare that they have no known competing financial interests or personal relationships that could have appeared to influence the work reported in this paper.

Data availability

Data will be made available on request.

Acknowledgments

References

Abdelhadi, O. M. A., Babiker, S. A., Bauchart, D., Listrat, A., Rémond, D., Hocquette, J. F., & Faye, B. (2017). Effect of gender on quality and nutritive value of dromedary camel (*Camelus dromedarius*) longissimus lumborum muscle. *Journal of the Saudi Society of Agricultural Sciences, 16*(3), 242–249. https://doi.org/10.1016/j.jssas.2015.08.003

Baba, W. N., Rasool, N., Selvamuthukumara, M., & Maqsood, S. (2021). A review on nutritional composition, health benefits, and technological interventions for improving consumer acceptability of camel meat: An ethnic food of Middle East. *Journal of Ethnic Foods, 8*(1), 18. https://doi.org/10.1186/s42779-021-00089-1

Cittadini, A., Domínguez, R., Pateiro, M., Sarriés, M. V., & Lorenzo, J. M. (2021). Fatty acid composition and volatile profile of *longissimus thoracis et lumborum* muscle from Burguete and Jaca Navarra foals fattened with different finishing diets. *Foods, 10*(12), 2914. https://doi.org/10.3390/foods10122914

Deng, S., Liu, Y., Huang, F., Liu, J., Han, D., Zhang, C., & Blecker, C. (2021). Evaluation of volatile flavor compounds in bacon made by different pig breeds during storage time. *Food Chemistry, 357*, Article 129765. https://doi.org/10.1016/j.foodchem.2021.129765

Drouin, G., Rioux, V., & Legrand, P. (2019). The n-3 docosapentaenoic acid (DPA): A new player in the n-3 long chain polyunsaturated fatty acid family. *Biochimie, 159*, 36–48. https://doi.org/10.1016/j.biochi.2019.01.022

Fang, Z., Li, G., Gu, Y., Wen, C., Ye, H., Ma, J., Liang, Z., Yang, L., Wu, J., & Chen, H. (2022). Flavour analysis of different varieties of camellia seed oil and the effect of the refining process on flavour substances. *LWT- Food Science and Technology, 170*, Article 114040. https://doi.org/10.1016/j.lwt.2022.114040

García-García, A. B., Lamichhane, S., Castejón, D., Cambero, M. I., & Bertram, H. C. (2018). 1H HR-MAS NMR-based metabolomics analysis for dry-fermented sausage characterization. *Food Chemistry, 240*, 514–523. https://doi.org/10.1016/j.foodchem.2017.07.150

Guo, X., Shi, D., Liu, C., Huang, Y., Wang, Q., Wang, J., Pei, L., & Lu, S. (2022). UPLC-MS-MS-based lipidomics for the evaluation of changes in lipids during dry-cured mutton ham processing. *Food Chemistry, 377*, Article 131977. https://doi.org/10.1016/j.foodchem.2021.131977

Hamed Hammad Mohammed, H., Jin, G., Ma, M., Khalifa, I., Shukat, R., Elkhedir, A. E., … Noman, A. E. (2020). Comparative characterization of proximate nutritional compositions, microbial quality and safety of camel meat in relation to mutton, beef, and chicken. *LWT- Food Science and Technology, 118*, Article 108714. https://doi.org/10.1016/j.lwt.2019.108714

Han, G., Zhang, L., Li, Q., Wang, Y., Chen, Q., & Kong, B. (2020). Impacts of different altitudes and natural drying times on lipolysis, lipid oxidation and flavour profile of traditional Tibetan yak jerky. *Meat Science, 162*, Article 108030. https://doi.org/10.1016/j.meatsci.2019.108030

Huang, Q., Dong, K., Wang, Q., Huang, X., Wang, G., An, F., Luo, Z., & Luo, P. (2022). Changes in volatile flavor of yak meat during oxidation based on multi-omics. *Food Chemistry, 371*, Article 131103. https://doi.org/10.1016/j.foodchem.2021.131103

Kadim, I. T., Al-Karousi, A., Mahgoub, O., Al-Marzooqi, W., Khalaf, S. K., Al-Maqbali, R. S., … Raiymbek, G. (2013). Chemical composition, quality and

histochemical characteristics of individual dromedary camel (*Camelus dromedarius*) muscles. *Meat Science, 93*(3), 564–571. https://doi.org/10.1016/j.meatsci.2012.11.028

Li, C., Li, X., Huang, Q., Zhuo, Y., Xu, B., & Wang, Z. (2020). Changes in the phospholipid molecular species in water-boiled salted duck during processing based on shotgun lipidomics. *Food Research International, 132*, Article 109064. https://doi.org/10.1016/j.foodres.2020.109064

Li, P., Zhou, H., Wang, Z., Al-Dalali, S., Nie, W., Xu, F., Li, C., Li, P., Cai, K., & Xu, B. (2022). Analysis of flavor formation during the production of Jinhua dry-cured ham using headspace-gas chromatography-ion mobility spectrometry (HS-GC-IMS). *Meat Science, 194*, Article 108992. https://doi.org/10.1016/j.meatsci.2022.108992

Li, R., Geng, C., Xiong, Z., Cui, Y., Liao, E., Peng, L., Jin, W., & Wang, H. (2022). Evaluation of protein degradation and flavor compounds during the processing of Xuan'en ham. *Journal of Food Science, 87*(8), 3366–3385. https://doi.org/10.1111/1750-3841.16242

Li, W., Wang, J., Zhang, C., Wang, N., Zhang, C., Chen, W., & Wu, T. (2023). Using an integrated feature-based molecular network and lipidomics approach to reveal the differential lipids in yak shanks and flanks. *Food Chemistry, 403*, Article 134352. https://doi.org/10.1016/j.foodchem.2022.134352

Li, W., Zheng, L., Xiao, Y., Li, L., Wang, N., Che, Z., & Wu, T. (2022). Insight into the aroma dynamics of Dongpo pork dish throughout the production process using electronic nose and GC×GC-MS. *LWT- Food Science and Technology, 169*, Article 113970. https://doi.org/10.1016/j.lwt.2022.113970

Liu, H., Hui, T., Zheng, X., Li, S., Wei, X., Li, P., Zhang, D., & Wang, Z. (2022). Characterization of key lipids for binding and generating aroma compounds in roasted mutton by UPLC-ESI-MS/MS and Orbitrap Exploris GC. *Food Chemistry, 374*, Article 131723. https://doi.org/10.1016/j.foodchem.2021.131723

Liu, H., Wang, Z., Zhang, D., Shen, Q., Pan, T., Hui, T., & Ma, J. (2019). Characterization of key aroma compounds in Beijing roasted duck by gas chromatography–Olfactometry–mass spectrometry, odor-activity values, and aroma-recombination experiments. *Journal of Agricultural and Food Chemistry, 67*(20), 5847–5856. https://doi.org/10.1021/acs.jafc.9b01564

Liu, Q., Lin, J., Zhao, W., Lei, M., Yang, J., & Bai, W. (2023). The dynamic changes of flavors and UPLC-Q-Exactive-Orbitrap-MS based lipidomics in mackerel (*Scomberomorus niphonius*) during dry-cured processing. *Food Research International, 163*, Article 112273. https://doi.org/10.1016/j.foodres.2022.112273

Liu, X., Liu, J., Yang, Z., Song, H., Liu, Y., & Zou, T. (2014). Aroma-active compounds in Jinhua ham produced with different fermentation periods. *Molecules, 19*(11), 19097–19113. https://www.mdpi.com/1420-3049/19/11/19097.

Lorenzo, J. M., & Carballo, J. (2015). Changes in physico-chemical properties and volatile compounds throughout the manufacturing process of dry-cured foal loin. *Meat Science, 99*, 44–51. https://doi.org/10.1016/j.meatsci.2014.08.013

Lv, J., Ma, J., Liu, Y., Li, P., Wang, D., Geng, Z., & Xu, W. (2023). Lipidomics analysis of Sanhuang chicken during cold storage reveals possible molecular mechanism of lipid changes. *Food Chemistry, 417*, Article 135914. https://doi.org/10.1016/j.foodchem.2023.135914

Man, L., Ren, W., Qin, H., Sun, M., Yuan, S., Zhu, M., Liu, G., Wang, C., & Li, M. (2023). Characterization of the relationship between lipids and volatile compounds in donkey, bovine, and sheep meat by UHPLC–ESI–MS and SPME–GC–MS. *LWT- Food Science and Technology, 175*, Article 114426. https://doi.org/10.1016/j.lwt.2023.114426

Narváez-Rivas, M., Gallardo, E., & León-Camacho, M. (2014). Chemical changes in volatile aldehydes and ketones from subcutaneous fat during ripening of Iberian dry-cured ham. Prediction of the curing time. *Food Research International, 55*, 381–390. https://doi.org/10.1016/j.foodres.2013.11.029

Poljanec, I., Marušić Radovčić, N., Petričević, S., Karolyi, D., Listeš, E., & Medić, H. (2021). Proteolysis and protein oxidation throughout the smoked dry-cured ham process. *Food Chemistry, 362*, Article 130207. https://doi.org/10.1016/j.foodchem.2021.130207

Siebers, M., Brands, M., Wewer, V., Duan, Y., Hölzl, G., & Dörmann, P. (2016). Lipids in plant–microbe interactions. *Biochimica et Biophysica Acta (BBA) - molecular and cell biology of. Lipids, 1861*(9, Part B), 1379–1395. https://doi.org/10.1016/j.bbalip.2016.02.021

Storrustløkken, L., Devle, H. M., Håseth, T. T., Egelandsdal, B., Naess-Andresen, C. F., Hollung, K., Berg, P., Ekeberg, D., & Alvseike, O. (2015). Lipid degradation and sensory characteristics of M. Biceps femoris in dry-cured hams from Duroc using three different processing methods. *International Journal of Food Science & Technology, 50*(2), 522–531. https://doi.org/10.1111/ijfs.12699

Tian, X., Li, Z. J., Chao, Y. Z., Wu, Z. Q., Zhou, M. X., Xiao, S. T., … Zhe, J. (2020). Evaluation by electronic tongue and headspace-GC-IMS analyses of the flavor compounds in dry-cured pork with different salt content. *Food Research International, 137*, Article 109456. https://doi.org/10.1016/j.foodres.2020.109456

van der Veen, J. N., Kennelly, J. P., Wan, S., Vance, J. E., Vance, D. E., & Jacobs, R. L. (2017). The critical role of phosphatidylcholine and phosphatidylethanolamine metabolism in health and disease. *Biochimica et Biophysica Acta (BBA) - Biomembranes, 1859*(9, Part B), 1558–1572. https://doi.org/10.1016/j.bbamem.2017.04.006

Wang, H., Wu, Y., Xiang, H., Sun-Waterhouse, D., Zhao, Y., Chen, S., Li, L., & Wang, Y. (2022). UHPLC-Q-Exactive Orbitrap MS/MS-based untargeted lipidomics reveals molecular mechanisms and metabolic pathways of lipid changes during golden pomfret (*Trachinotus ovatus*) fermentation. *Food Chemistry, 396*, Article 133676. https://doi.org/10.1016/j.foodchem.2022.133676

Wang, P., Zhong, L., Yang, H., Zhang, J., Hou, X., Wu, C., Zhang, R., & Cheng, Y. (2022). Comprehensive comparative analysis of lipid profile in dried and fresh walnut kernels by UHPLC-Q-Exactive Orbitrap/MS. *Food Chemistry, 386*, Article 132706. https://doi.org/10.1016/j.foodchem.2022.132706

Wang, Z., Nie, T., Zhang, H., Wang, W., Chen, H., Wang, S., & Sun, B. (2023). Correlation analysis between volatile compounds and quality attributes in pork tenderloin in response to different stir-frying processes. *Foods, 12*(23), 4299. https://doi.org/10.3390/foods12234299

Xu, C., Yu, H., Xie, P., Sun, B., Wang, X., & Zhang, S. (2020). Influence of electrostatic field on the quality attributes and volatile flavor compounds of dry-cured beef during chill storage. *Foods, 9*(4), 478. https://doi.org/10.3390/foods9040478

Xu, P., Liu, L., Liu, K., Wang, J., Gao, R., Zhao, Y., Bai, F., Li, Y., Wu, J., Zeng, M., & Xu, X. (2023). Flavor formation analysis based on sensory profiles and lipidomics of unrinsed mixed sturgeon surimi gels. *Food Chemistry: X, 17*, Article 100534. https://doi.org/10.1016/j.fochx.2022.100534

Yang, Z., Chen, G., Liao, G., Zheng, Z., Zhong, Y., & Wang, G. (2023). UHPLC-MS/MS-based lipidomics for the evaluation of the relationship between lipid changes and Zn-protoporphyrin formation during Nuodeng ham processing. *Food Research International, 174*, Article 113509. https://doi.org/10.1016/j.foodres.2023.113509

Zhang, M., Fu, J., Mao, J., Dong, X., & Chen, Y. (2023). Lipidomics reveals the relationship between lipid oxidation and flavor formation of basic amnio acids participated low-sodium cured large yellow croaker. *Food Chemistry, 429*, Article 136888. https://doi.org/10.1016/j.foodchem.2023.136888

Zhang, Q., Ding, Y., Gu, S., Zhu, S., Zhou, X., & Ding, Y. (2020). Identification of changes in volatile compounds in dry-cured fish during storage using HS-GC-IMS. *Food Research International, 137*, Article 109339. https://doi.org/10.1016/j.foodres.2020.109339

Zhang, Q., Wan, C., Wang, C., Chen, H., Liu, Y., Li, S., Lin, D., Wu, D., & Qin, W. (2018). Evaluation of the non-aldehyde volatile compounds formed during deep-fat frying process. *Food Chemistry, 243*, 151–161. https://doi.org/10.1016/j.foodchem.2017.09.121

Zhao, X., Cheng, X., Zang, M., Wang, L., Li, X., Yue, Y., & Liu, B. (2022). Insights into the characteristics and molecular transformation of lipids in Litopenaeus vannamei during drying from combined lipidomics. *Journal of Food Composition and Analysis, 114*, Article 104809. https://doi.org/10.1016/j.jfca.2022.104809

Zhou, Y., Wang, X., Chen, Y., & Yuan, B. (2021). Effects of different paprikas on the quality characteristics and volatile flavor components of spiced beef. *Journal of Food Processing and Preservation, 45*(4), Article e15353. https://doi.org/10.1111/jfpp.15353